MAPPING 3D STRUCTURE OF URBAN TREES USING AIRBORNE LIDAR DATA FOR TOPOGRAPHIC SURVEY

H. Oshio*, T. Asawa

School of Environment and Society, Tokyo Institute of Technology, Yokohama, Japan – (oshio.h.aa, asawa.t.aa)@m.titech.ac.jp

KEY WORDS: Airborne LiDAR, Leaf area density, Urban area, Vegetation, Voxel.

ABSTRACT:

The designing of urban spaces utilizing trees is a promising approach to alleviate the severe thermal environment. Three-dimensional (3D) information on individual trees is important for their maintenance and for evaluating their microclimatic effects. Methods have been developed for estimating the 3D distribution of leaf area density (LAD) using high-density airborne light detection and ranging (LiDAR) point cloud. However, the coverage of high-density data is limited. This study sought to develop a method for estimating LAD distribution using existing low-density LiDAR data that was obtained for the nationwide topographic survey. A point cloud with the same density as the existing data was generated from the high-density data. LAD was estimated using the generated point cloud and was compared with LAD derived from the high-density data and terrestrial LiDAR to clarify the spatial scale of information obtained from the existing data. A method to improve the spatial scale was also examined. These methods were applied to the actual existing LiDAR data to generate a 3D information map at an urban scale.

1. INTRODUCTION

The designing of urban spaces utilizing trees is a promising approach to alleviate the severe thermal environment. Three-dimensional information on individual trees is important for their maintenance and for evaluating their microclimatic effects. The leaf area density (LAD) distribution is a key index for characterizing the vertical and horizontal crown structures (Iio et al., 2007; Whitehead et al. 1990) and is defined as the total one-sided leaf area per unit volume with a unit of m^2 m^{-3}. Methods for estimating LAD have been developed using high-density point clouds (~20 incident beams per square meter) derived from airborne light detection and ranging (LiDAR) (Arnqvist et al., 2020; de Almeida et al., 2019; Halubok et al., 2022; Oshio et al., 2015). However, the cost of obtaining such data makes the method applicable only in limited regions. Information over a wider area is necessary to evaluate the impact of trees on urban climate and assess the carbon fixation of urban trees.

Therefore, we focused on existing data such as airborne LiDAR data obtained for the nationwide topographic survey by the national institution that is responsible for surveying the land. Although the density of such data is several points per square meter, it would be practical if this data could be used to estimate 3D tree structure. In this paper, we sought to develop a method for estimating LAD distribution using existing low-density LiDAR data that was obtained for the nationwide topographic survey. The spatial scale of information obtained from the existing data was examined. Subsequently, a method to improve the spatial scale was investigated. Then, the method was applied to the actual data over city areas to generate a 3D tree structure map.

Date	July–August, 2007
Laser beam divergence	0.28 mrad
Scan angle	±10°
Flight altitude	2000 m
Swath	700 m
Foot print diameter	0.56 m
Point density	2.5 points (single and first return) /m^2 (overlapped area)
Number of returns per pulse	4

Table 1. Specifications of GSI low-density LiDAR data.

Date	September 6, 2010
Observation system	SAKURA (Heliborne system, Nakanihon Air Service)
Scanner	LMS-Q560 (RIEGL)
Wave length	1550 nm
Laser beam divergence	0.5 mrad
Ranging accuracy	20 mm
Range resolution	0.5 m
Scan angle	±22.5°
Flight altitude	350 m
Swath	290 m
Foot print diameter	0.175 m
Point density	20 points (single and first return) /m^2
Number of returns per pulse	Unlimited (actual max in the data: 5)

Table 2. Specifications of high-density LiDAR data.

* Corresponding author

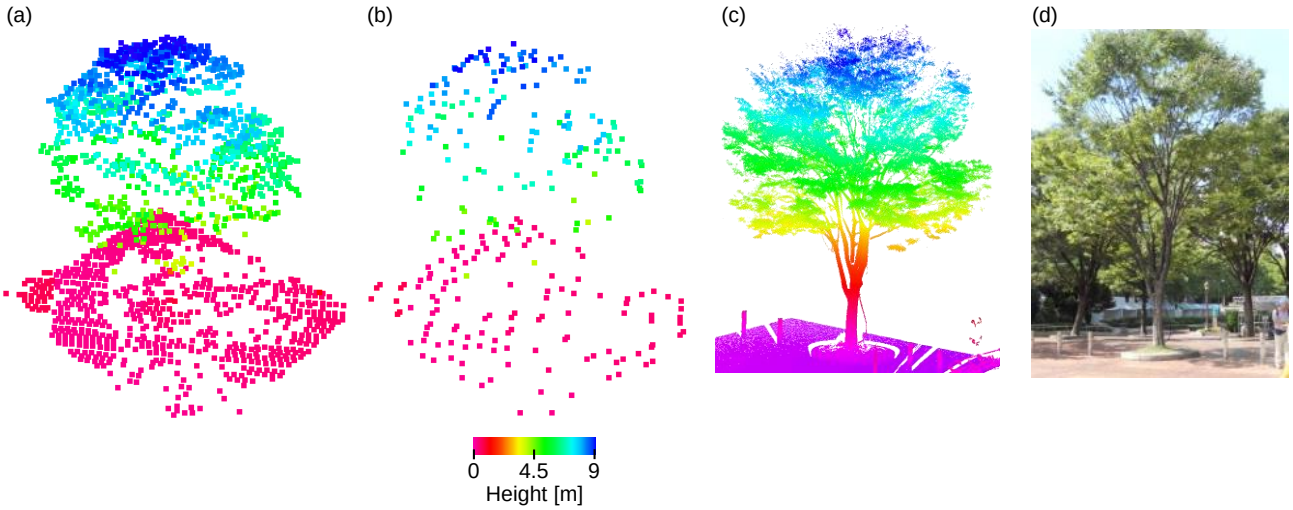

Figure 1. Point cloud of the target *Z. serrata*: (a) high-density airborne LiDAR; (b) generated low-density data; (c) terrestrial LiDAR; (d) photograph taken on the ground.

2. DATA AND PROCESSING

2.1 Low-Density Existing LiDAR Data

The data used was airborne LiDAR data acquired by the Geospatial Information Authority of Japan (GSI) to generate a 5-m mesh digital terrain model of all of Japan. Assuming that the results of the research will be used in urban planning and urban development, data from Yokohama City, which focuses on the preservation and creation of green spaces and is the location of our laboratory, was used. Table 1 shows the specifications of the data.

2.2 High-Density LiDAR Data

Unfortunately, the truth data (accurate and the same time period) to compare with the GSI low-density data was not available; therefore, low-density data was generated from high-density airborne LiDAR data that had corresponding terrestrial LiDAR data. A Method for estimating LAD was investigated using the generated low-density data, and the developed method was applied to the GSI low-density data from Yokohama City. The high-density airborne LiDAR data for Hisaya-Odori Street in Nagoya, Japan was used. This data was acquired on September 6, 2010, during which time there were leaf-on conditions in Japan. A helicopter-based laser scanning system (Nakanihon Air Service, Nishikasugai, Japan) with an LMSQ560 sensor (RIEGL Laser Measurement Systems GmbH, Horn, Austria) was used for the observation. The specifications of the data are shown in Table 2.

From that data, we employed a point cloud of *Z. serrata* with a height of 10.5 m and with average leaf density (Figure 1). Terrestrial LiDAR measurements were carried out on September 2, 2010. The *Z. serrata* was scanned from two positions 10 m away from the tree using a terrestrial laser scanner (VZ-400; RIEGL Laser Measurement Systems GmbH, Horn, Austria). The increments of the zenith and azimuth angles of the laser beam emission were 0.04°, yielding a point spacing of 7 mm on a vertical plane 10 m ahead. The details of high-density airborne LiDAR data and terrestrial LiDAR data are provided in Oshio et al. (2015).

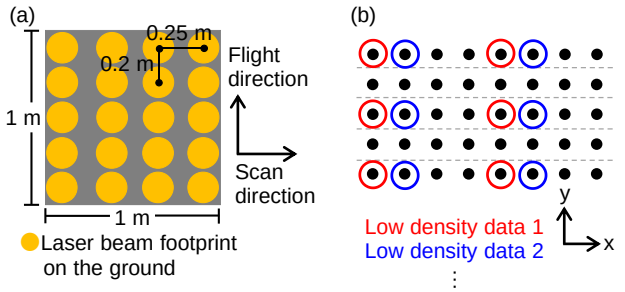

Figure 2. Schematic of the method to generate low-density data: (a) laser beam incident pattern of the high-density data: (b) extracting points from high-density data.

The LAD of the *Z. serrata* was obtained using a previously proposed method (Hosoi and Omasa, 2006; Oshio and Asawa, 2020). The terrestrial LiDAR-derived LAD of the *Z. serrata* was used to verify the accuracy of LAD estimated using the generated low-density data.

2.3 Generation of Low-Density Data

A schematic figure of the airborne laser beam incident pattern is shown in Figure 2(a). Although the actual point distribution was irregular, the low-density data was generated as shown in Figure 2(b). Figure 2(b) represents single and first return points viewed from above. In a coordinate system where the x-axis points in the scan direction, the data were divided at 0.2 m intervals in the y direction (broken line in Figure 2(b)). Then, one point for every four points in the x direction and one point for every two points in the y direction was extracted, yielding eight low-density point clouds. The last and intermediate return points were distributed to the point cloud that contained the corresponding first return point. Point clouds with a large difference in density from GSI data or with an extremely small number of intermediate returns were excluded from the analysis, and four point clouds were used in subsequent analyses. A generated low-density point cloud of the *Z. serrata* is shown in Figure 1(b).

For each generated low-density point cloud, LAD was estimated using the method of Oshio et al. (2015) for different voxel sizes (0.5 m, 1 m, 2 m, and 4 m). The method is based on the

relationship between LAD and the contact frequency between leaves and laser beams. The contact frequency was calculated by tracing the paths of laser beams. If there were multiple returns for a incident beam, all return points were considered in the calculation.

3. COMPARISON OF LAD BETWEEN LOW-DENSITY DATA AND TERRESTRIAL LIDAR

The LAD estimated using the generated low-density data was compared with that derived from terrestrial LiDAR. Only voxels with a laser beam incident ratio of terrestrial LiDAR higher than 0.8 were used for comparison to ensure the accuracy of terrestrial LiDAR-derived LAD. Laser beam incident ratio is the ratio of the number of laser beams actually incident on the voxel to the number of laser beams that would be incident if beams were not intercepted by leaves and branches before reaching the voxel. Both numbers were obtained by tracing the paths of laser beams.

Figure 3 shows the variation in the filled ratio with the voxel size. The filled ratio is the fraction of voxels with low-density data-derived LAD greater than zero among voxels with terrestrial LiDAR-derived LAD greater than zero. As can be predicted from the point density, the 0.5m voxel cannot represent the distribution of leaves in low-density data. Even for 1 m voxel, more than half of voxels with terrestrial LAD > 0 did not contain low-density points. For the voxel size of 2 m, the filled ratio was close to 0.8, and the difference from the results for the voxel size of 4 m was small.

Figure 4 shows the variation in the mean absolute difference in LAD between low-density data and terrestrial LiDAR with the voxel size. The absolute value of the difference in LAD between low-density data and terrestrial LiDAR was calculated for each voxel, and the mean for all voxels was obtained. As in the case of the filled ratio, the difference was small when the voxel size was 2 m, and the difference from the results for the voxel size of 4 m was also small. Then, it was concluded that the spatial scale of the LAD obtained from the low-density data was 2 m.

4. IMPROVING SPATIAL SCLAE OF LOW-DENSITY DATA-DERIVED LAD

When the voxel size is 2 m, the error in the absorbed radiation obtained using the radiative transfer simulation is large (Oshio and Asawa, 2023). The shaded area is also greatly overestimated for the voxel size of 2 m (Figure 5). In Figure 5, the terrestrial LiDAR point cloud of the *Z. serrata* was voxelized at different sizes and was projected onto the ground surface from the solar direction. Three different solar zenith angles were used. Inside the shaded area was filled in (i.e., if ground pixels on which no voxels were projected were surrounded by shaded pixels, these pixels were treated as shaded pixels). From the above, a method to improve voxel size from 2 m to 1 m was investigated.

Assuming the distribution of leaves within a voxel is related to the distribution of surrounding leaves, a method using LAD of the surrounding voxels was tested. Figure 6 shows the schematic of the method. For each of the eight 1 m voxels within a 2 m voxel, a weight was calculated according to the LAD and distance of the adjacent 2 m voxels as

$$w_i = \sum_{j=1}^{7} \frac{\rho_j}{{r_{ij}}^2} \quad (1)$$

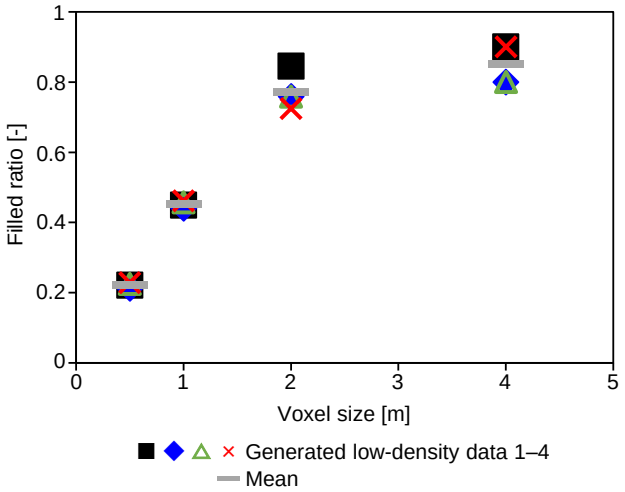

Figure 3. Variation in the filled ratio with voxel size.

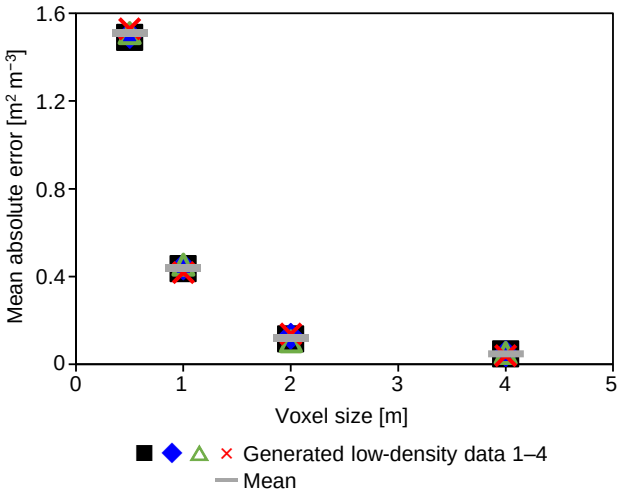

Figure 4. Variation in the mean absolute error in LAD with voxel size

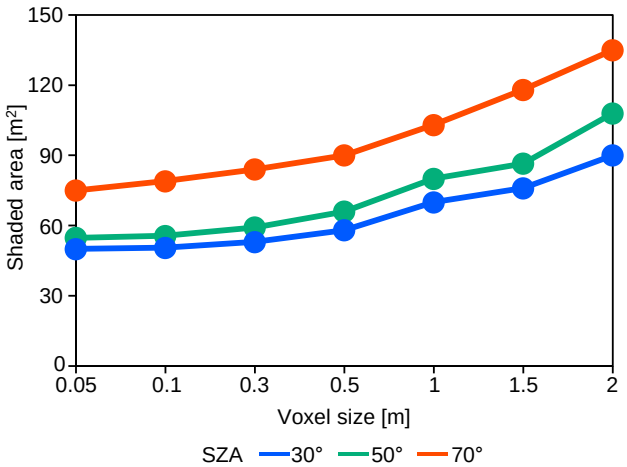

Figure 5. Variation in the shaded area provided by the *Z. serrata* with voxel size and solar zenith angle (SZA).

where w_i is the weight for ith 1m voxel (i=1–8), ρ_j is the LAD of jth surrounding 2 m voxel, and r_{ij} is the distance between the center of ith 1m voxel and that of jth surrounding 2m voxel. Then, the leaf area of the 2 m voxel was distributed to the 1 m voxels that were included within the 2 m voxel and had a weight greater than a threshold value. The distribution was made in proportion to the weight. The threshold value was determined by comparison with the terrestrial LiDAR data.

The refined LAD with 1 m voxel was compared with the terrestrial LiDAR-derived LAD with 1 m voxel. The fraction of correct, omission, and commission voxels are shown in Figure 7. Correct indicates the refined LAD > 0 for the voxel with terrestrial LiDAR-derived LAD > 0. Omission indicates the refined LAD = 0 for the voxel with terrestrial LiDAR-derived LAD > 0. Commission indicates the refined LAD > 0 for the voxel with terrestrial LiDAR-derived LAD = 0. According to Figure 7(a), the fraction of omission voxel was high for the lower part of the crown. However, in the intermediate height area of the tree crown where the amount of leaves was large, the fraction of correct voxel was high. For the entire tree crown, the fraction of the correct voxel was about 0.7, which was comparable to the results for high-density data with 1 m voxels (Oshio et al., 2015). Similar to Oshio et al. (2015), a certain percentage of omission voxels were considered to have small LAD that were difficult to detect by airborne LiDAR.

A comparison between the refined LAD and the terrestrial LiDAR-derived LAD is shown in Figure 8. Although there was a large variation in the scatter plot, in voxels where the terrestrial LiDAR-derived LAD was large, the refined LAD showed a certain degree of large value. The mean absolute error in LAD was 0.3–0.4 m^2 m^{-3}. This was not small compared to the mean of the terrestrial LiDAR-derived LAD for the entire crown (0.58 m^2 m^{-3}). However, the relative difference in total crown leaf area between the generated low-density data and terrestrial LiDAR was 12%. Therefore, further study on how to distribute leaves in a 2 m voxel into 1 m voxels would improve accuracy.

5. GENERATING 3D MAP FROM GSI DATA

A 2 km × 2 km area, which included Odori Park and Nogeyama Park on the west side of the Kannai district, was cut out from the GSI LiDAR data for Yokohama City. Tree points were manually extracted from the data. This process is expected to be automated using recent AI technology (Liu et al., 2013; Shinohara et al., 2020; Shinohara et al., 2021; Zhou and Neumann, 2013). The 1 m voxel LAD distribution was estimated using the method discussed in previous sections. The point cloud of buildings was also divided into 1 m voxels. Figure 9 shows the LAD distribution map. This map provides information on the three-dimensional amount of greenery that could not be obtained from the conventional green cover distribution map, as well as the differences in tree shape and leaf density depending on tree species and growth conditions. The voxel-based information can be applied to numerical simulations to evaluate the thermal and wind environments of streets (Oshio et al., 2021; Grylls and Reeuwijk, 2021).

6. CONCLUSIONS

The spatial scale of LAD distribution obtained from a low-density point cloud (~2.5 incident beams per square meter) was 2 m. A method to improve the spatial scale to 1 m was investigated. For the distribution of voxels with LAD > 0, the refined data agreed well with the terrestrial LiDAR. There was a certain correlation between the LAD values of the refined data

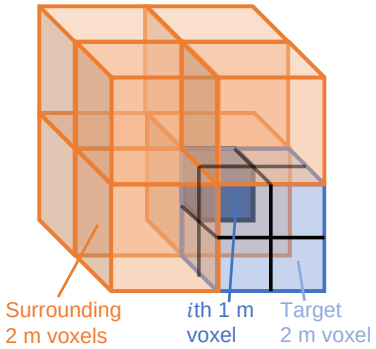

Figure 6. Schematic of the method to improve LAD spatial scale.

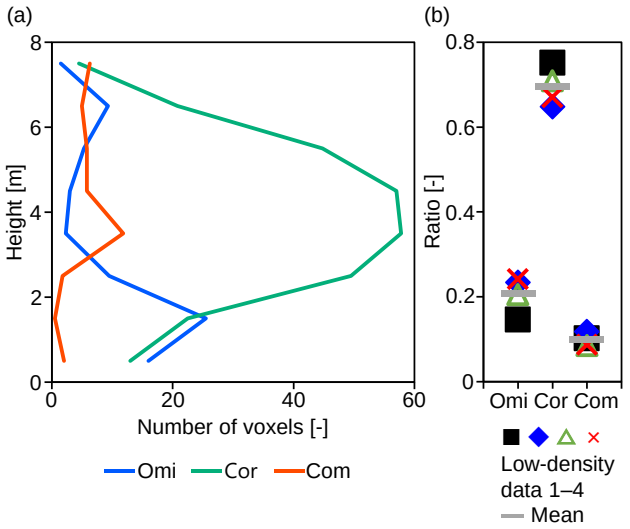

Figure 7. Evaluation of correct (Cor), omission (Omi), and commission (Com) voxels for the refined LAD with 1 m voxels: (a) vertical distribution of number of voxels (mean of four data); (b) ratio for the entire crown.

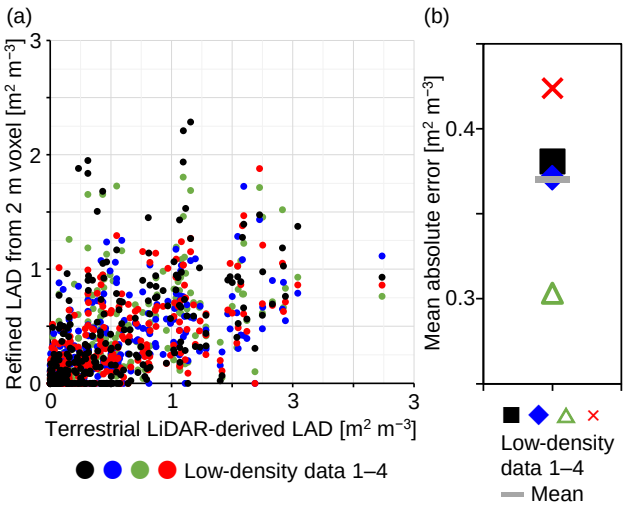

Figure 8. Comparison between low-density data-derived refined LAD and terrestrial LiDAR-derived LAD: (a) scatter plot; (b) mean absolute error.

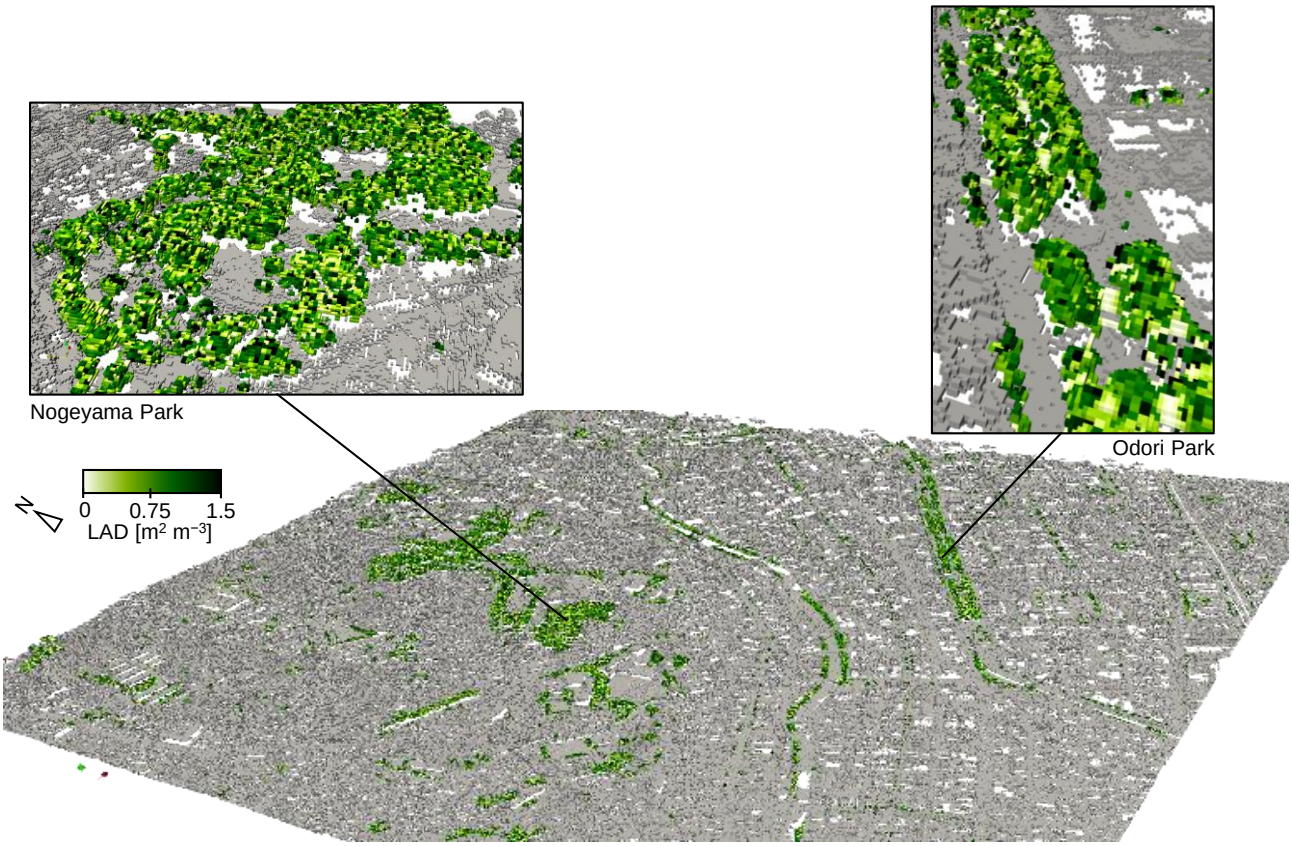

Figure 9. 3D tree structure map for a 2 km × 2 km area in Yokohama City.

and terrestrial LiDAR; however, the absolute error in LAD was about 60% of the mean LAD value of the tree. The method to distribute leaves in a 2 m voxel into 1 m voxels needs to be improved. The proposed method was applied to the actual GSI low-density LiDAR data, and a 3D tree structure map was generated. In the future, this map will be used to evaluate the thermal and wind environments of urban areas to confirm its effectiveness.

ACKNOWLEDGEMENTS

The low-density LiDAR data for Yokohama City was provided by GSI. The high-density airborne LiDAR data was offered by S. Miyasaka (Nakanihon Air Service Company, Ltd.). Part of this study was conducted as a graduation thesis research for Mr. Naoki Kouya (then an undergraduate student at Tokyo Institute of Technology).

REFERENCES

Arnqvist, J., Freier, J., Dellwik, E., 2020: Robust processing of airborne laser scans to plant area density profiles. *Biogeosciences*, 17, 5939-5952. doi.org/10.5194/bg-17-5939-2020.

de Almeida, D.R.A., Stark, S.C., Shao, G., Schietti, J., Nelson, B.W., Silva, C.A., Gorgens, E.B., Valbuena, R., Papa, D. de A., Brancalion, P.H.S., 2019: Optimizing the remote detection of tropical rainforest structure with airborne lidar: leaf area profile sensitivity to pulse density and spatial sampling. *Remote Sensing*, 11, 92. doi.org/10.3390/rs11010092.

Grylls, T., Reeuwijk, M., 2021: Tree model with drag, transpiration, shading and deposition: Identification of cooling regimes and large-eddy simulation. *Agr. Forest Meteorol.*, 298-299, 108288. doi.org/10.1016/j.agrformet.2020.108288.

Halubok, M., Kochanski, A.K., Stoll, R., Bailey, B.N., 2022: Errors in the estimation of leaf area density from aerial LiDAR data: influence of statistical sampling and heterogeneity. *IEEE T. Geosci. Remote Sens.*, 60, 4407314. doi.org/10.1109/TGRS.2021.3123585.

Hosoi, F., Omasa, K., 2006: Voxel-Based 3-D Modeling of Individual Trees for estimating leaf area density using high-resolution portable scanning lidar. *IEEE T. Geosci. Remote Sens.*, 44, 3610-3618. doi.org/10.1109/TGRS.2006.881743.

Iio, A., Kakubari, Y., Mizunaga, H., 2011: A three-dimensional light transfer model based on the vertical point-quadrant method and Monte-Carlo simulation in a Faguscrenata forest canopy on Mount Naeba in Japan. *Agr. Forest Meteorol.*, 151, 461-479. doi.org/10.1016/j.agrformet.2010.12.003.

Liu, J., Shen, J., Zhao, R., Xu, S., 2013: Extraction of individual tree crowns from airborne LiDAR data in human settlements. *Math. Comput. Model.*, 58, 524-535. doi.org/10.1016/j.mcm.2011.10.071.

Oshio, H., Asawa, T., 2020: Verifying the accuracy of the leaf area density distribution of an individual tree derived from terrestrial laser scanning while considering the penetration of beams into the crown and the influence of wind. *J. Remote Sens. Soc. Japan*, 40, S34-S43. doi.org/10.11440/rssj.40.S34.

Oshio, H., Asawa, T., 2023: Simulating the 3D distribution of absorbed shortwave radiation in a tree crown: comparison of simplified and monte carlo models. *J. Geophys. Res.-Atmos.*, 128, e2023JD038612. doi.org/10.1029/2023JD038612.

Oshio, H., Asawa, T., Hoyano, A., Miyasaka, S., 2015: Estimation of the leaf area density distribution of individual trees using high-resolution and multi-return airborne LiDAR data. *Remote Sens. Environ.*, 166, 116-125. doi.org/10.1016/j.rse. 2015.05.001.

Oshio, H., Kiyono, T., Asawa, T., 2021: Numerical simulation of the nocturnal cooling effect of urban trees considering the leaf area density distribution. *Urban For. Urban Gree.*, 66, 127391. doi.org/10.1016/j.ufug.2021.127391.

Shinohara, T., Xiu, H., Matsuoka, M., 2020: FWNet: semantic segmentation for full-waveform LiDAR data using deep learning. *Sensors*, 20, 3568. doi.org/10.3390/s20123568.

Shinohara, T., Xiu, H., Matsuoka, M., 2021: Point2Wave: 3-D point cloud to waveform translation using a conditional generative adversarial network with dual discriminators. *IEEE J. Sel. Top. Appl.*, 14, 11630-11642. doi.org/10.1109/JSTARS. 2021.3124610.

Whitehead, D., Grace, J.C., Godfrey, M.J.S., 1990: Architectural distribution of foliage in individual Pinus radiata D. Don crowns and the effects of clumping on radiation interception. *Tree Physiol.*, 7, 135-155. doi.org/10.1093/treephys/7.1-2-3-4.135.

Zhou, Q.-Y., Neumann, U., 2013: Complete residential urban area reconstruction from dense aerial LiDAR point clouds. *Graph. Models*, 75, 118-125. doi.org/ 10.1016/j.gmod.2012.09.001.